Journal Pre-Proof

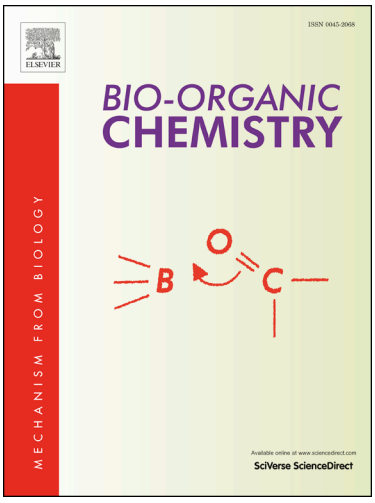

Synthesis, biological evaluation and molecular docking studies of bis-chalcone derivatives as xanthine oxidase inhibitors and anticancer agents

Serdar Burmaoglu, Seyda Ozcan, Sevgi Balcioglu, Melis Gencel, Samir Abbas Ali Noma, Sebnem Essiz, Burhan Ates, Oztekin Algul

PII: S0045-2068(19)30350-5
DOI: https://doi.org/10.1016/j.bioorg.2019.103149
Reference: YBIOO 103149

To appear in: *Bioorganic Chemistry*

Received Date: 3 March 2019
Revised Date: 9 July 2019
Accepted Date: 23 July 2019

Please cite this article as: S. Burmaoglu, S. Ozcan, S. Balcioglu, M. Gencel, S. Abbas Ali Noma, S. Essiz, B. Ates, O. Algul, Synthesis, biological evaluation and molecular docking studies of bis-chalcone derivatives as xanthine oxidase inhibitors and anticancer agents, *Bioorganic Chemistry* (2019), doi: https://doi.org/10.1016/j.bioorg.2019.103149

This is a PDF file of an article that has undergone enhancements after acceptance, such as the addition of a cover page and metadata, and formatting for readability, but it is not yet the definitive version of record. This version will undergo additional copyediting, typesetting and review before it is published in its final form, but we are providing this version to give early visibility of the article. Please note that, during the production process, errors may be discovered which could affect the content, and all legal disclaimers that apply to the journal pertain.

© 2019 Published by Elsevier Inc.

JOURNAL PRE-PROOF

Synthesis, biological evaluation and molecular docking studies of bis-chalcone derivatives as xanthine oxidase inhibitors and anticancer agents

Serdar Burmaoglu[a,b]*, Seyda Ozcan[b], Sevgi Balcioglu[c], Melis Gencel[d], Samir Abbas Ali Noma[c], Sebnem Essiz[d], Burhan Ates[c], Oztekin Algul[e]*

[a]*Tercan Vocational High School, Erzincan Binali Yildirim University, Erzincan 24800, Turkey*

[b]*Deparment of Chemistry, Faculty of Science, Ataturk University, Erzurum 25240, Turkey*

[c]*Department of Chemistry, Faculty of Science and Arts, İnönü University, Malatya 44280, Turkey*

[d]*Bioinformatics and Genetics Department, Faculty of Engineering and Natural Sciences, Kadir Has University, Istanbul 34083, Turkey*

[e]*Department of Pharmaceutical Chemistry, Faculty of Pharmacy, Mersin University, Mersin 33169, Turkey.*

∗Corresponding authors. Tel.: +90-324-341-2815; fax: +90-324-341-3022; e-mail: oztekinalgul@mersin.edu.tr (OA), Tel.: +90-446-441-3627; fax: +90-446-441-3672; e-mail: sburmaoglu@erzincan.edu.tr (SB). *These authors contributed equally.

JOURNAL PRE-PROOF

ABSTRACT

In this study, a series of B-ring fluoro substituted bis-chalcone derivatives were synthesized by Claisen-Schmidt condensation reactions and evaluated for their ability to inhibit xanthine oxidase (XO) and growth inhibitory activity against MCF-7 and Caco-2 human cancer cell lines, *in vitro*. According to the results obtained, the bis-chalcone with fluoro group at the 2 (**4b**) or 2,5-position (**4g**) of B-ring were found to be potent inhibitors of the enzyme with IC_{50} values in the low micromolar range. The effects of these compounds were about 7 fold higher than allopurinol. The binding modes of the bis-chalcone derivatives in the active site of xanthine oxidase were explained using molecular docking calculations. Also, compound **4g** and **4h** showed *in vitro* growth inhibitory activity against a panel of two human cancer cell lines 1,9 and 6.8 μM of IC_{50} values, respectively.

Keywords: Bis-chalcone, synthesis, Claisen-Schmidt condensation, inhibition, cytotoxicity

GRAPHICAL ABSTRACT:

HIGHLIGHTS:

- Eight bis-chalcone derivatives were synthesized by Claisen-Schmidt condensation reaction.
- Target compounds were assessed *in vitro* against MCF-7 and Caco-2 tumor cell lines.
- Target compounds were evaluated for their ability to inhibit xanthine oxidase.
- Molecular Modeling studies have been carried out.

JOURNAL PRE-PROOF

1. Introduction

Cancer is one of the most challenging diseases that have been struggled despite the many clinical and basic studies conducted on it over the years. It is reported that the chance of cytotoxic agents to destroy tumor cells in convential chemotherapy is higher than compared with normal cells. However, since these agents do not have too much specificity, they may result in systemic toxicity caused by undesirable side effects. Therefore, obtaining novel anticancer agents specific to tumor would be a move to significantly improve the efficacy of cancer chemotherapy [1].

In recent years, numerous FDA-supported fluorine-containing compounds come to the fore, indicating that fluorine atom plays an important role in medical chemistry, chemical biology and drug discovery. In the current studies of drug design and discovery, the fluorine atom is the second most favourite hetero atom after nitrogen. Replacement of a C-H or C-O bond with a C-F bond on a biologically active molecule has been reported to generally show many desired pharmacological properties such as metabolic stability, binding to target molecules, and enhanced membrane permeability. Moreover, the properties that make fluorine appealing may include the small atomic radius, high electronegativity and low polarization of the C-F bond [2]. In light of all this information, it can be said that the anticancer agents containing fluorine can act as targeted molecular missile warheads [1].

The chalcones are simple-structure compounds found in the structure of many natural products and have a very wide distribution in vegetables, fruits, teas and many other plants. The chalcones have always aroused researchers' interest not only from synthetic or biosynthetic point of view, but also due to their interesting biological characteristics. Because the therapeutic applications of chalcones by means of using plants and medicinal herbs have been utilized in conventional medicine to treat numerous diseases, such as cancer, inflammation and diabetes, for thousands of years [3].

Several compounds in the chalcone structure have been approved for their clinical use. Figure 1 illustrates the structures of metochalcone, once sold as a choleretic drug, and sofalcone compounds used as anti-ulcer and mucoprotective drugs [3].

JOURNAL PRE-PROOF

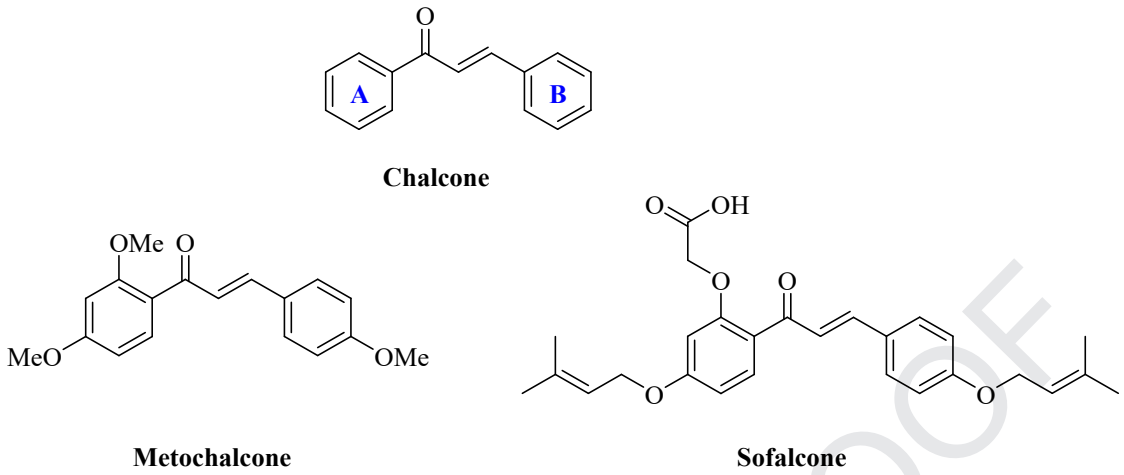

Figure 1. Structures of chalcone and two clinically approved chalcone-based drugs.

The compounds containing two chalcone units in a single structure are called bis-chalcones. The bis-chalcones also exhibit a broad variety of biological properties. Some bis-chalcone analogs have been reported to be potent NO production inhibitors and cytotoxic agents against four human cancer cell lines (A549, DU145, KB and KB-VIN) [4]. The biphenyl-based bis-chalcones have been reported to have an anticancer activity against MCF-7 and MDA-MB 231 human breast cancer, HeLa, human embryonic kidney (HEK-293) cells [5].

XO is an enzyme that plays a role in the degradation of purines. During the degradation process of purines, XO produces reactive oxygen species (ROS). The excess activity of XO can lead to oxidative stress, mutagenesis and possibly cancer. In addition, inhibition of XO causes to reduced oxidative stress and subsequently to reduced inflammation and reduced tissue wasting and improved outcome during treatment of disease. Therefore, the inhibition of XO might be strategy for cancer therapy [6,7].

The aim of this study was to investigate the compounds obtained by strategically including the fluorine atom in the compounds in the bis-chalcone structure in terms of anticancer and XO inhibition. For this, XO inhibition activity studies and cytotoxic properties on MCF-7 and Caco-2 cancer cells lines were conducted by synthesizing a series of bis-chalcone derivatives containing fluorine in different positions of both B-rings. The general structure of synthesized compounds is shown in Figure 2.

JOURNAL PRE-PROOF

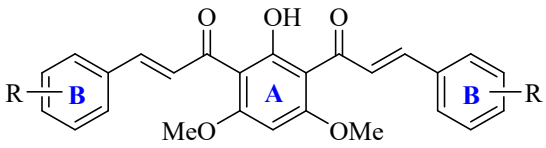

bis-chalcone

Figure 2. General structure of bis-chalcone.

2. Results and discussion

2.1. Synthesis of bis-chalcone derivatives

Compound **2** was prepared from trimethoxybenzene (**1**) and acetyl chloride in the presence of $AlCl_3$. Bis-chalcones were prepared from compound **2** and appropriate benzaldehydes (**3a-h**) in the presence of 50% KOH solution in MeOH (Scheme 1). After a standard work-up (addition of NH_4Cl solution and extraction with ethyl acetate), the resulting solid was purified by column chromatography to yield the desired products.

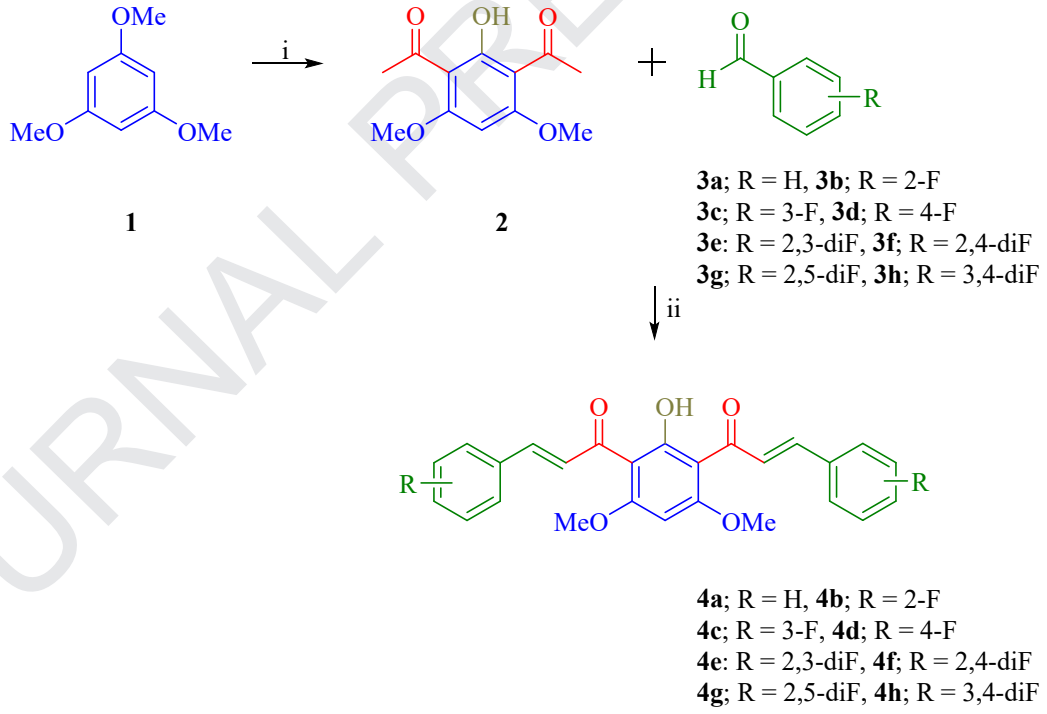

Scheme 1. General synthetic method. Reagents; (i) CH_3COCl, $AlCl_3$; (ii) 50% KOH, MeOH, rt.

JOURNAL PRE-PROOF

JOURNAL PRE-PROOF

2.2. Cytotoxicity Evaluation

The cytotoxicity evaluation of the compounds was performed by MTT test against MCF-7 and Caco-2 cell lines. Cisplatin was used as standard for comparison. As shown in Figure 3 and Figure 4, all complexes showed much higher cytotoxicity than Cisplatin against Caco-2 and MCF-7 cell lines. As seen from the Figure 3, compound **4g** showed the best IC_{50} value against MCF-7 cell line as 1.9 μM which is at least three-fold higher than the other compounds. Furthermore, among all complexes, **4a** and **4b** showed higher toxicity than **4c**, **4d**, **4e**, **4f** and **4h**. Compound **4g** showed the lowest toxicity result against MCF-7 cell line as 103.7 μM. Figure 4 shows the toxicity values of the compounds against Caco-2 cell line. In this cell line, results are generally parallel to MCF-7. Also, compound **4g** and **4h** showed the highest toxicity, and compound **4d** and **4e** showed the lowest toxicity. Generally, there are no major differences between cell lines in terms of toxicity of the compounds, indicating that there is no cell specific toxicity. The images monitored by invert microscope at the end of 24 h confirmed the results (Figure 5, 6, 7 and 8, see supplementary information). The morphological changes in MCF-7 cells after treatment with **4g** for 24 h demonstrated that cell confluent level dramatically decreased in compared with the other compounds (Figure 5 and 6, see supplementary information). In addition, growth rate of Caco-2 cell from the morphological images is parallel with IC_{50} values (Figure 7 and 8, see supplementary information).

Although more detailed studies are needed to understand the mechanism of action, except for compound **4e**, high cytotoxicity results of the compounds make them a promising candidate for the treatment of colorectal and breast cancer.

JOURNAL PRE-PROOF

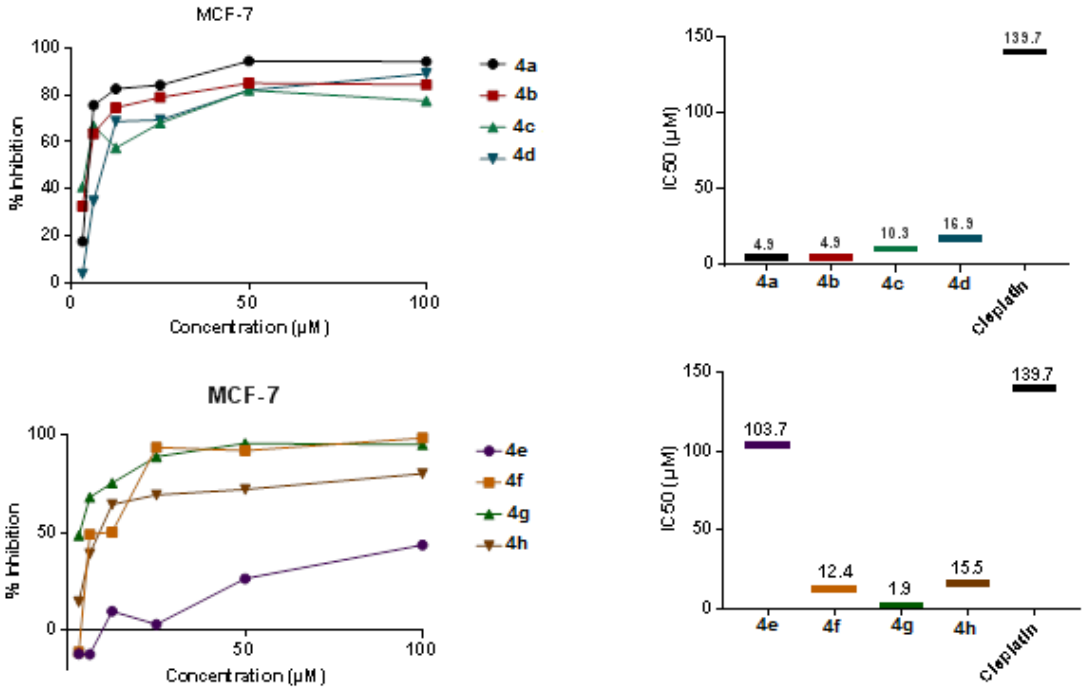

Figure 3. % Inhibition graphics and IC_{50} values of the compounds against MCF-7 cell line.

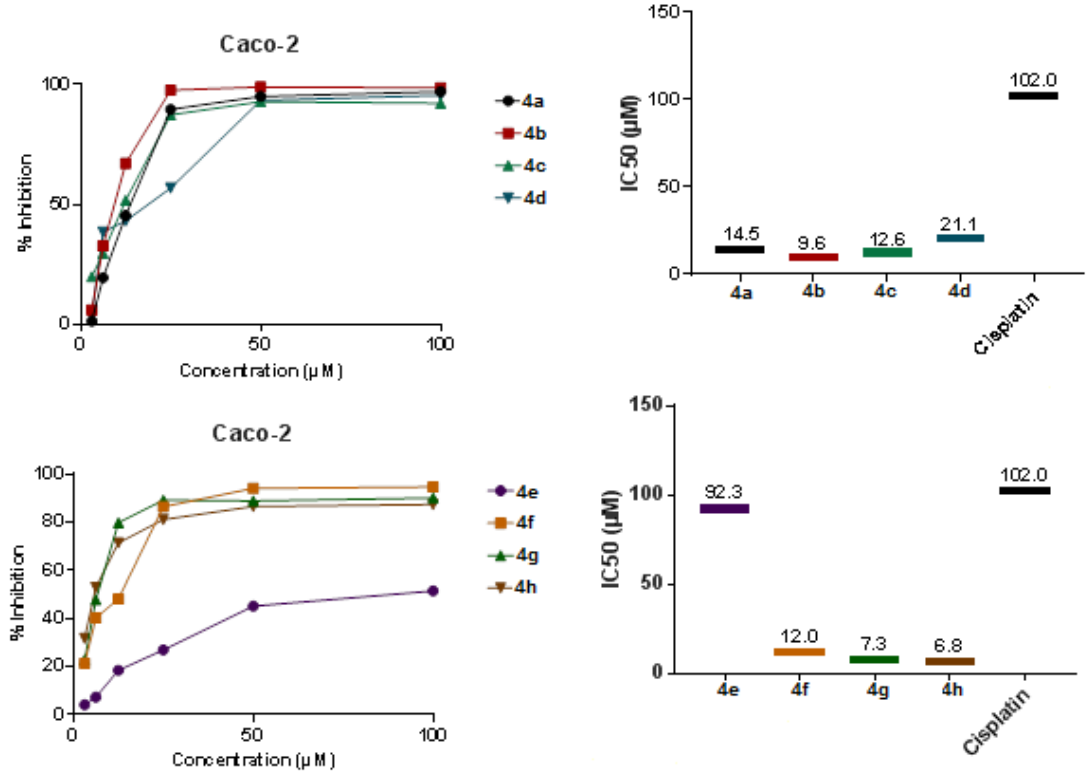

Figure 4. % Inhibition and IC_{50} values of the compounds against Caco-2 cell line.

2.3. Xanthine Oxidase (XO) Inhibitory Activity

The experimental results indicated that all the compounds showed remarkable inhibition activity toward XO as compared with the standard allopurinol. In this study, we investigated the XO inhibitor effects of eight different compounds, the results are given as half maximal inhibitory micromolar concentrations (IC_{50}) values calculated by equation prepared from the different concentrations of compounds. All compounds showed inhibition behaviour on XO enzyme. The range of IC_{50} value for XO inhibition was determined from (0.728-6.058 μM) as shown in (Table 1). Compound **4b** showed the lowest IC_{50} value as 0.728 μM while compound **4c** showed the highest IC_{50} value as 6.058 μM. The IC_{50} for allopurinol was determined 5.43 μM as a positive control. In addition, compounds **4a**, **4b**, **4d**, and **4g** have non-competitive inhibition, while compounds **4c**, **4e**, **4f**, and **4h** have competitive inhibition like allopurinol (Table 1). It means that non-competitive inhibition is effective mechanism in the low IC_{50} values compared with competitive inhibition.

In a previous study, the range of IC_{50} value for XO inhibition was determined from 4.608 to 7.084 μM for some pyrrole carboxamide derivatives by Kibriz *et al*. [8]. In other study, Zhang *et al*. founded the range from (6.7-45 μM) for seventeen compounds of benzonitrile derivatives as IC_{50} value for XO inhibition [9]. Nile *et al*., investigated natural plant flavonoids effect on XO enzyme and found IC_{50} range between (4.5-21.3 μg/mL) [10]. According to our results, all compounds exhibited more inhibition activity than allopurinol except for compounds **4c** and **4e**. In addition, **4b** and **4g** have almost 7-fold higher inhibition activity on XO than allopurinol.

JOURNAL PRE-PROOF

Table 1. The IC_{50} values and inhibition types of the compounds on XO activity.

Compound No	IC_{50} (µM)	r^2	Type of Inhibition
4a	2.010 ± 0.046	0.938	Non-competitive
4b	0.728 ± 0.009	0.980	Non-competitive
4c	6.058 ± 0.095	0.993	Competitive
4d	3.592 ± 0.044	0.904	Non-competitive
4e	5.516 ± 0.077	0.999	Competitive
4f	4.001 ± 0.089	0.997	Competitive
4g	0.764 ± 0.008	0.954	Non-competitive
4h	3.995 ± 0.059	0.993	Competitive
Allopurinol	5.430 ± 0.029	0.986	Competitive

2.4. Binding pose analyses

In Figure 9A, the binding pose of quercetin and in Figure 9B the binding pose of salicylic acid are inspected. X-Ray conformations are displayed on the left column and docked positions are displayed on the right column. Also, RMSD of the best docked position from crystalized ligand is calculated. The RMSD values for quercetin and salicylic acid are 0.9 Å and 1.2 Å, respectively. If the RMSD is lower than 2Å, docking process count as successful [11]. The visual and RMSD inspection of the binding site and known binding poses validated that docking scoring function is able to pick the correct pose for these molecules.

Before moving to the compounds of this study, allopurinol and oxypurinol which are clinically known inhibitors of XO, are also docked to the binding site, and their binding energies are 4.48 ± 0.01 and 6.60 ± 0.00 kcal/mol, respectively.

JOURNAL PRE-PROOF

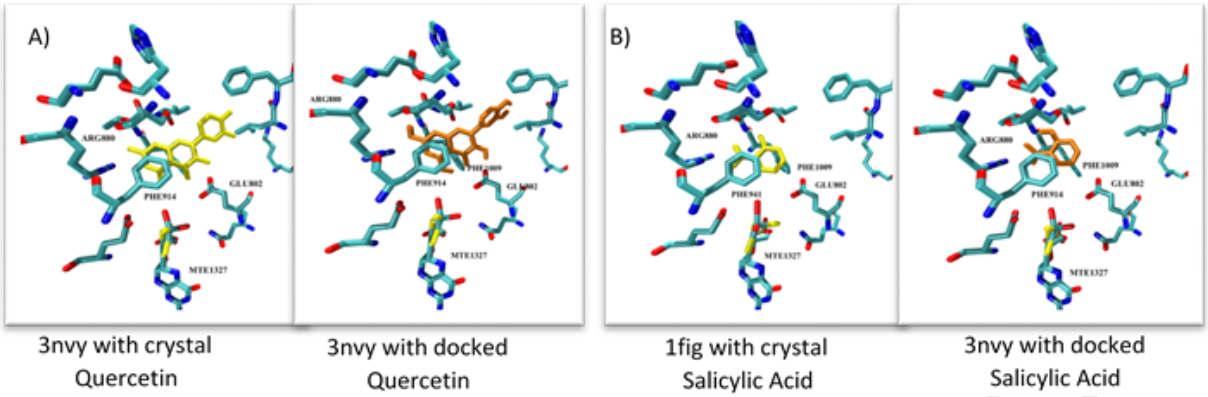

Figure 9. X-Ray (yellow) and docked (orange) positions A) Quercetin and B) Salicylic Acid.

All eight compounds showed similar binding poses and their binding energies range from -9.8 kcal/mol to -8.8 kcal/mol which are all better than oxy or allopurinol binding energies. Three dominant interaction poses observed are summarized in Table 2 with their corresponding binding energies. In Figure 10 panels A, B and C, the binding energy of each compound is displayed in the graph with the pose on the bottom of the panel respectively for the three poses.

Table 2. Binding energies of each pose and percentage of the pose observed in 1000 conformations.

Compounds	Lowest Binding Energies (kcal/mol)			Number in Cluster (1000 run)		
	Pose 1	Pose 2	Pose 3	Pose 1	Pose 2	Pose 3
4a	-9.82±0.05	-8.55±0.01	-8.44±0.01	24%	24%	29%
4b	-9.70±0.02	-8.84±0.05	-8.54±0.01	25%	24%	24%
4c	-9.83±0.03	-8.63±0.04	-8.49±0.01	29%	24%	22%
4d	-9.11±0.04	-8.54±0.08	-7.90±0.06	29%	23%	3%
4e	-9.80±0.04	-8.76±0.03	-8.60±0.02	28%	21%	19%
4f	-8.98±0.05	-8.63±0.05	-8.17±0.09	33%	23%	5%
4g	-9.70±0.09	-8.83±0.04	-8.44±0.03	26%	22%	19%
4h	-9.30±0.05	-8.47±0.04	-7.98±0.04	30%	21%	3%

Namely, first pose is the cluster which contains the lowest binding energy conformation for each compound (Figure 10 A). Bis-chalcone derivatives show a T-shaped π-π stacking interaction with PHE1009 (Figure 10 B and C). This interaction is shown to be important in substrate binding and activation [12]. Another T-shaped π-π interaction is seen between ligand and PHE649 in addition to three hydrogen bonds between ligand and protein residues ASN768, LYS771, GLU802 (Figure 10 B and C). In this pose, compounds **4c**, **4e** and **4g** display the lowest binding energy (Figure 10 A).

The second pose of the compounds (Figure 10 E and H) shows single T-shaped π-π stacking with PHE1009 and three hydrogen bonds with ASN768, LYS771, GLU802 residues. Formation of halogen bond between; amino group of LYS771 with compounds of **4e** and **4g** and hydroxyl group of THR1010 with compound **4e** has been observed. Binding energies for this pose varies between -8.84 to -8.47 kcal/mol (Figure 10B).

When pose 3 is considered, it resembles a pose similar to pose 1. Both of the phenyl rings are curved though binding pocket. One of the phenyl rings is sandwiched between PHE1009 and PHE914 and makes parallel π-π stacking with PHE914. Two hydrogen bonds are recognized between molecules and target protein (GLU802, SER876). Hydroxyl group of THR1010 forms a halogen bond to compound **4h**, carboxyl group of GLU802 forms halogen bond with **4b** and **4g**. For pose 2 and 3, the binding energy shows a similar trend, namely compounds **4b**, **4e** and **4g** show lowest binding energies (Figure 10 B and C respectively).

JOURNAL PRE-PROOF

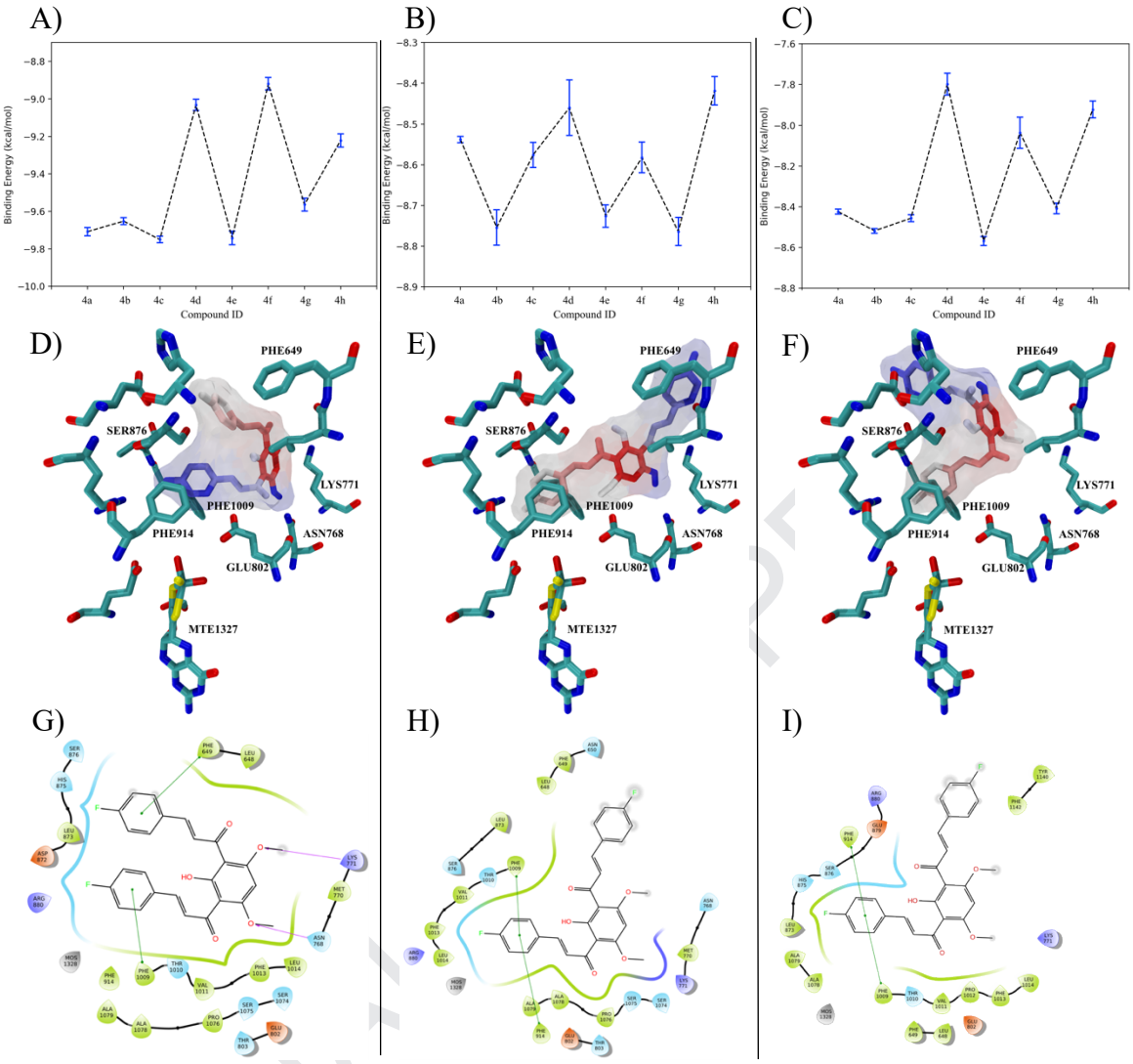

Figure 10. Binding Free Energies for eight compounds A) Pose 1, B) Pose 2, C) Pose 3. 3D view of each pose in binding site D) Pose 1, E) Pose 2, F) Pose 3 (Pictures were prepared using VMD) [13]. 2D interaction graphs of each pose G) Pose 1, H) Pose 2, I) Pose 3 (2D interaction maps were taken from Maestro) [14]. Compound **4d** was used as a representation in figures.

3. Conclusions

Two series of bis-chalcone functionalized in B-ring were synthesized to evaluate their effects as inhibitors of xanthine oxidase and anticancer activities. Eight bis-chalcone derivatives were synthesized by Claisen-Schmidt condensation reactions. The bis-chalcone

with substituted at 2- and 2,5- position (compounds **4b** and **4g**) were found to be more potent as compared to the other substituted derivatives **4a**, **4c**, **4d**, **4e**, **4f** and 4 h. The nature of substituents at the 3- and 4-position of compounds **4c**, **4d**, and disubstituted compounds **4e**, **4f** and **4h** do not influence sufficiently their inhibitory activity. Docking of inhibitors to the active site of XO allows to explain possible binding modes of the two groups of bis-chalcone derivatives.

There is generally a compatibility between enzyme inhibition assay and docking results. Molecules **4b**, **4e** and **4g** which form a halogen bond, in addition to the other interaction types, displayed stronger binding in general. Only compound **4e** results showed some incompatibility. This is due to problems with the dissolution of compound **4e** *in vitro* enzyme inhibition studies. Structure-activity relationship analysis in conjunction with molecular docking indicated that the most active XO inhibitors carried a minimum of one fluoro group in 2 position. These data reveal that fluoro substituted bis-chalcone scaffold may be useful for designing new inhibitors that target XO.

In parallel, the ability of the synthesized bis-chalcones to cytotoxicity was determined. *In vitro* activity of the compounds was performed by MTT test agains MCF-7 and Caco-2 cell lines. Compound **4g** showed the best IC_{50} value against MCF-7 (1.9 μM) and **4g** and **4h** showed for Caco-2 cell line as 7.3 and 6.8 μM, respectively. Also, compound **4g** and **4h** showed the highest toxicity, and the images monitored by invert microscope at the end of 24 h confirmed the results. These results provided an important basis for further optimization of compound **4g** as a potential anticancer agent.

In the future, it is planned to carry out the designs for the solution of the existing dissolution problem in the compounds and to reveal the mechanisms of actions.

4. Experimental Part

4.1. General

All reagents used were commercially available unless otherwise specified. Melting points were measured with Gallenkamp melting point devices. IR Spectra: PerkinElmer Spectrum One FT-IR spectrometer. ^{1}H- and ^{13}C-NMR Spectra: Varian 400 and Bruker 400 spectrometers. Elemental analysis results were obtained on a Leco CHNS-932 instrument.

*4.1.1. 1,1'-(2-hydroxy-4,6-dimethoxy-1,3-phenylene)diethanone (**2**)*

To a solution of trimethoxybenzene (**1**) (5 g, 29.72 mmol) in DCM (50 mL) $AlCl_3$ (12.209 g, 91.56 mmol) and acetyl chloride (6.15 mL 86.50 mmol) were added sequentially and stirred at -15 °C for 1,5 h. The reaction was then allowed to warm to room temperature and stirred for an additional 20 h at this temperature. Completion of reaction was monitored by TLC analysis. After that, water (50 mL) was slowly added to the mixture at 0 °C. The mixture was then extracted with DCM (3 x 100 mL). The combined extracts were dried over Na_2SO_4 and the solvent was removed in vacuo. The crude product purified via coloumn chromatography over silica gel using gradient elution with EtOAc and hexanes to yield compound **2** as a white solid (55% yield). **^{1}H NMR** (400 MHz, $CDCl_3$) δ 14.20 (s, 1H), 5.93 (s, 1H), 3.89 (s, 6H), 2.53 (s, 6H). The ^{1}H NMR spectrum is in agreement with the reported data of [15].

*4.1.2. General procedure for preparation of bis-chalcones (**4a-h**)*

To a solution of compound **2** in MeOH (30 mL/1 mmol of substrate) benzaldehyde derivatives (**3a-h**) (3 eq) and 50% KOH solution (15 mL/1 mmol of substrate) were added sequentially and stirred for 24 h at room temperature. Completion of reaction was monitored by TLC analysis. The resulting mixture was concentrated in vacuo, diluted with NH_4Cl solution (50 mL) and extracted with ethyl acetate (2 x 50 mL). The organic layer was dried over Na_2SO_4 and concentrated in vacuo. The residual solid was purified by column chromatography to yield the desired products.

*4.1.3. (2E,2'E)-1,1'-(2-hydroxy-4,6-dimethoxy-1,3-phenylene)bis(3-phenylprop-2-en-1-one) (**4a**)*

The above general procedure was followed with benzaldehyde (**3a**) to yield **4a** as a dark yellow solid (62% yield). **R_f** (EtOAc/Hexanes 60:40) = 0,50; **mp** = 163-164 °C; **^{1}H NMR** (400 MHz, $CDCl_3$) δ 14.26 (s, 1H), 7.64 (d, 2H, *J* = 15.8 Hz), 7.61 – 7.53 (m, 6H), 7.45 (d, 2H, *J* = 15.8 Hz), 7.41 – 7.34 (m, 4H), 6.06 (s, 1H), 3.97 (s, 6H); **^{13}C NMR** (100 MHz, $CDCl_3$) δ 193.2, 164.8, 163.9, 143.9, 135.4, 130.5, 129.1, 128.7, 128.1, 108.9, 86.8, 56.2; **Anal. calcd** for $C_{26}H_{22}O_5$: C, 75.35; H, 5.35; Found: C,75.75; H, 5.36.

JOURNAL PRE-PROOF

*4.1.4. (2E,2'E)-1,1'-(2-hydroxy-4,6-dimethoxy-1,3-phenylene)bis(3-(2-fluorophenyl)prop-2-en-1-one) (**4b**)*

The above general procedure was followed with 2-fluorobenzaldehyde (**3b**) to yield **4b** as a dark yellow solid (90% yield). **R_f** (EtOAc/Hexanes 60:40) = 0,53; **mp** = 139-140 °C; **^{1}H NMR** (400 MHz, $CDCl_3$) δ 14.27 (s, 1H), 7.74 (d, 2H, *J* = 16.0 Hz), 7.59 (t, 2H, *J* = 7.6 Hz), 7.54 (d, 2H, *J* = 16.0 Hz), 7.35 (dd, 2H, *J* = 13.6, 5.6 Hz), 7.17 (t, 2H, *J* = 7.6 Hz), 7.12 – 7.05 (m, 2H), 6.05 (s, 1H), 3.96 (s, 6H); **^{13}C NMR** (100 MHz, $CDCl_3$) δ 193.1, 164.9, 164.1, 163.1, 160.5, 136.3, 131.9, 131.8, 130.5, 130.5, 129.8, 129.7, 124.7, 124.6, 123.5, 123.4, 116.5, 116.3, 108.8, 86.8, 56.2; **Anal. calcd** for $C_{26}H_{20}F_2O_5$: C, 69.33; H, 4.48; Found: C,69.42; H, 4.75.

*4.1.5. (2E,2'E)-1,1'-(2-hydroxy-4,6-dimethoxy-1,3-phenylene)bis(3-(3-fluorophenyl)prop-2-en-1-one) (**4c**)*

The above general procedure was followed with 3-fluorobenzaldehyde (**3c**) to yield **4c** as a dark yellow solid (99% yield). **R_f** (EtOAc/Hexanes 60:40) = 0,56; **mp** = 175-176 °C; **^{1}H NMR** (400 MHz, $CDCl_3$) δ 14.29 (s,1H), 7.56 (d, 2H, *J* = 15.8 Hz), 7.40 (d, 2H, *J* = 15.8 Hz), 7.36 – 7.29 (m, 4H), 7.27 – 7.21 (m, 2H), 7.10 – 7.01 (m, 2H), 6.05 (s, 1H), 3.96 (s,6H); **^{13}C NMR** (100 MHz, $CDCl_3$) δ 192.8, 164.9, 164.4, 164.1, 161.9, 142.2, 142.2, 137.6, 137.6, 130.7, 130.6, 129.2, 124.8, 124.7, 117.4, 117.2, 114.8, 114.6, 108.7, 86.9, 86.8, 56.3, 56.3; **Anal. calcd** for $C_{26}H_{20}F_2O_5$: C, 69.33; H, 4.48; Found: C, 69.37; H, 4.68.

*4.1.6. (2E,2'E)-1,1'-(2-hydroxy-4,6-dimethoxy-1,3-phenylene)bis(3-(4-fluorophenyl)prop-2-en-1-one) (**4d**)*

The above general procedure was followed with 4-fluorobenzaldehyde (**3d**) to yield **4d** as a dark yellow solid (78% yield). **R_f** (EtOAc/Hexanes 60:40) = 0,53; **mp** = 177-178 °C; **^{1}H NMR** (400 MHz, $CDCl_3$) δ 14.33 (s, 1H), 7.61 – 7.50 (m, 6H), 7.35 (d, 2H, *J* = 15.8 Hz), 7.07 (t, 4H, *J* = 8.6 Hz), 6.05 (s, 1H), 3.95 (s, 6H); **^{13}C NMR** (100 MHz, $CDCl_3$) δ 192.9, 165.4, 164.8, 163.9, 162.9, 142.6, 131.6, 131.5, 130.6, 130.5, 127.8, 116.3, 116.1, 108.8, 86.9, 86.8, 56.3, 56.2; **Anal. calcd** for $C_{26}H_{20}F_2O_5$: C, 69.33; H, 4.48; Found: C, 69.42; H, 4.69.

*4.1.7. (2E,2'E)-1,1'-(2-hydroxy-4,6-dimethoxy-1,3-phenylene)bis(3-(2,3-difluorophenyl)prop-2-en-1-one) (**4e**)*

The above general procedure was followed with 2,3-difluorobenzaldehyde (3e) to yield 4e as a dark yellow solid (90% yield). R_f (EtOAc/Hexanes 60:40) = 0,33; mp = 215-216 °C; ^{1}H NMR (400 MHz, $CDCl_3$) δ 14.22 (s, 1H), 7.69 (d, 2H, *J* = 16.0 Hz), 7.55 (d, 2H, *J* = 16.1 Hz), 7.34 (s, 2H), 7.24 – 7.03 (m, 4H), 6.06 (s, 1H), 3.97 (s, 6H); ^{13}C NMR (100 MHz, $CDCl_3$) δ 192.7, 165.1, 164.3, 134.9, 131.7, 131.6, 125.8, 124.6, 124.5, 124.5, 118.7, 118.5, 108.7, 86.8, 56.2; Anal. calcd for $C_{26}H_{18}F_4O_5$: C, 64.20; H, 3.73; Found: C, 64.57; H, 4.11.

*4.1.8. (2E,2'E)-1,1'-(2-hydroxy-4,6-dimethoxy-1,3-phenylene)bis(3-(2,4-difluorophenyl)prop-2-en-1-one) (**4f**)*

The above general procedure was followed with 2,4-difluorobenzaldehyde (**3f**) to yield **4f** as a dark yellow solid (74% yield). **R_f** (EtOAc/Hexanes 60:40) = 0,46; **mp** = 177-178 °C; **^{1}H NMR** (400 MHz, $CDCl_3$) δ 14.28 (s, 1H), 7.67 (d, 2H, *J* = 16.0 Hz, A part of AB system), 7.58 (dd, 2H, *J* = 15.0, 8.4 Hz), 7.47 (d, 2H, *J* = 16.1 Hz, B part of AB), 6.87 (ddd, 4H, *J* = 21.8, 13.8, 5.3 Hz), 6.04 (s, 1H), 3.95 (s, 6H); **^{13}C NMR** (100 MHz, $CDCl_3$) δ 192.8, 165.4, 165.3, 164.9, 164.1, 163.4, 163.3, 162.9, 162.8, 160.8, 160.7, 135.2, 130.9, 130.9, 130.8, 130.8, 130.0, 129.9, 120.0, 119.9, 112.4, 112.4, 112.2, 112.1, 108.7, 105.1, 104.8, 104.6, 86.8, 56.2; **Anal. calcd** for $C_{26}H_{18}F_4O_5$: C, 64.20; H, 3.73; Found: C, 64.45; H, 3.95.

*4.1.9. (2E,2'E)-1,1'-(2-hydroxy-4,6-dimethoxy-1,3-phenylene)bis(3-(2,5-difluorophenyl)prop-2-en-1-one) (**4g**)*

The above general procedure was followed with 2,5-difluorobenzaldehyde (**3g**) to yield **4g** as a dark yellow solid (99% yield). **R_f** (EtOAc/Hexanes 60:40) = 0,60; **mp** = 166-167 °C; **^{1}H NMR** (400 MHz, $CDCl_3$) δ 14.24 (s,1H), 7.66 (d, 2H, *J* = 16.0 Hz), 7.47 (d, 2H, *J* = 16.0 Hz), 7.32 – 7.16 (m, 2H), 7.10 – 6.89 (m, 4H), 6.04 (s,1H), 3.96 (s, 6H); **^{13}C NMR** (100 MHz, $CDCl_3$) δ 192.5, 176.0, 165.1, 164.3, 160.1, 159.0, 157.7, 156.5, 134.7, 131.3, 131.2, 124.8, 124.7, 124.7, 124.6, 118.4, 118.3, 118.1, 118.1, 117.7, 117.6, 117.4, 117.4, 115.2, 115.2, 114.9, 108.6, 86.9, 86.9, 56.3, 56.2; **Anal. calcd** for $C_{26}H_{18}F_4O_5$: C, 64.20; H, 3.73; Found: C, 64.21; H, 4.03.

*4.1.10.(2E,2'E)-1,1'-(2-hydroxy-4,6-dimethoxy-1,3-phenylene)bis(3-(3,4-difluorophenyl)prop-2-en-1-one) (**4h**)*

The above general procedure was followed with 3,4-difluorobenzaldehyde (**3h**) to yield **4h** as a dark yellow solid (80% yield). **R_f** (EtOAc/Hexanes 60:40) = 0,43; **mp** = 211-212 °C; **^{1}H NMR** (400 MHz, $CDCl_3$) δ 14.26 (s, 1H), 7.52 (d, 2H, *J* = 15.8 Hz), 7.44 – 7.37 (m, 2H), 7.33 (d, 2H, *J* = 15.8 Hz), 7.28 (d, 2H, *J* = 2.2 Hz), 7.17 (dd, 2H, *J* = 18.0, 8.3 Hz), 6.05 (s, 1H), 3.97 (s, 6H); **^{13}C NMR** (100 MHz, $CDCl_3$) δ 192.4, 164.9, 164.1, 153.0, 152.9, 152.1, 151.9, 150.5, 150.4, 149.6, 149.5, 141.2, 132.7, 132.6, 132.6, 128.9, 128.9, 125.5, 125.5, 125.4, 125.4, 118.1, 117.9, 116.7, 116.6, 108.7, 86.8, 56.3; **Anal. calcd** for $C_{26}H_{18}F_4O_5$: C, 64.20; H, 3.73; Found: C, 64.26; H, 3.90.

4.2. Cytotoxicity Studies

The cytotoxicity of the compounds was evaluated by MTT (3- (4,5-Dimethylthiazol-2-yl) -2,5-Diphenyltetrazolium Bromide) test. MCF-7 (human breast adenocarcinoma) and Caco-2 (human colorectal adenocarcinoma) cell lines were used in the study. First, cells were incubated with DMEM medium at 37 °C under 5% CO_2 until being 80% confluent. Then, the cells were removed from the surface by trypsin and counted with Thoma counting chamber and seeded in 96 well plates as $7x10^3$ cells/well. Next, plates were incubated under the same conditions for 24 h and the medium was replaced with compound solutions prepared with media (including less than 1% DMSO) at the certain concentrations (3.125, 6.25, 12.5, 25, 50 and 100 μM for each cell type). After incubating the plates 24 h under the same conditions, the compound solutions were then removed from the plates and 90 μL of DMEM and 10 μL of MTT (5 mg/mL in PBS, pH 7.4) were added and incubated for 4 h under the same conditions. At the end of the period, the MTT solution was removed followed by adding 100 μL of DMSO and the absorbance at 550 nm with a microplate reader was measured. Control wells were considered as 100% viable and IC_{50} of each compound was calculated by the linear curve of concentration vs % inhibiton graphics [16].

4.3. In vitro Assay of Xanthine Oxidase (XO) Inhibitory Activity

In vitro bovine XO inhibitory activity was performed spectrophotometrically by measuring the uric acid formation at 295 nm at 37 °C. In order to determinate IC_{50} value for XO inhibition, the compounds at different concentrations were added to the reaction

mixture and the absorbance was measured at 295 nm. The assayed method was based on the procedure reported by Sweeney a. P. *et al*. [17]. For enzyme assay, 50 mM of phosphate buffer (pH = 7.5), 1 mM of xanthine, and 0.2 U of XO enzyme were used. The enzymes were pre-incubated for 10 min, with tested compounds, then the reaction was started by addition xanthine to the reaction mixture. The tested compounds were dissolved in DMSO, then diluted with phosphate buffer, the final concentration of DMSO in the reaction mixture was less than 0.01% v/v which is not an interference value with enzyme assay [18]. All the experiments were performed in triplicates, and values were expressed as means of three experiments. Allopurinol was used as a positive control. The IC_{50} values of compounds were determined by using the percent inhibition of XO. The percent inhibition of XO activity was calculated as the following formula:

% Inhibition = (A-B)/A×100

where A = the absorbance at 295 nm without the test compound,

B = the absorbance at 295 nm with the test compound.

4.4. Molecular Modelling

The three dimensional (3D) structures of ligands were drawn by using the chemical modeling software Avogadro [19]. Geometry optimization tool embedded in Avogadro was used for structural refinement and small molecules were minimized using MMF94x force field [20].

In order to theoretically investigate the potency and binding pose of these eight molecules, Autodock molecular docking software was used [21]. The coordinates of the protein were obtained from PDB databank, 3NVY [22]. This structure of XO at 2 Å resolution contains quercetin molecule in its binding site. First quercetin and water molecules were removed and the catalytic part of the protein was prepared with the molybdenum metal ions (Mo) and cofactor MTE (phosphoric acid mono 2-amino-5,6-dimercapto-4-oxo-3,7,8a,9,10,10a-hexahydro-4H-8-oxa-1,3,9,10-tetraaza-anthracen-7-yl methyl).

To create coordinate, grid box and docking parameter files, AutoDockTool was used [21]. Gasteiger partial charges were assigned to each atom. Autodock 4.2 was used for grid

mapping and docking [21]. Energy Grid box was arranged as 50 × 50 × 50 × Å and its center was taken according to its native ligand center. To search for all conformations, Lamarckian genetic algorithm was applied [23]. For each ligand 1000 runs were performed using the population size of 300, 10.000.000 million energy evaluations, and the maximum of 27000 generations to span all the conformational space. From resulting 1000 docked positions, the poses are ranked according to the binding energy obtained from AutoDock 4.2. For the eight bis-chalcone derivatives, three best scored docking clusters are displayed in the results section. Docked conformers are clustered according to their Root Mean Square Deviation (RMSD). All molecular graphics material was prepared using VMD [13].

For an initial validation study of the binding site, quercetin and salicylic molecules were re-docked to the prepared binding site. Best-scoring docked pose of the molecules obtained from the software was checked against X-ray crystal orientation and conformation of the ligand. This is often referred to as the "bound" docking problem [24]. Additionally, allopurinol and oxypurinol known inhibitors of XO, were also docked to the prepared binding site for calculating reference binding energy values.

Acknowledgements

We thank the Scientific and Technological Research Council of Turkey (TUBITAK. Grant Number: 114Z554).

Appendix A. Supplementary material

Supplementary data to this article can be found online at

References

[1] J. Seitz, J. G. Vineberg, E. S. Zuniga, I. Ojima, J. Fluor. Chem. 152 (2013) 157.

[2] I. Ojima, J. Fluor. Chem. 198 **(**2017) 10.

[3] C. Zhuang, W. Zhang, C. Sheng, W. Zhang, C. Xing, Z. Miao, Chem. Rev. 117 (2017) 7762.

[4] M. V. B. Reddy, Y. Shen, E. Ohkoshi, K. F. Bastow, K. Qian, K. Lee, T. Wu, Eur. J. Med. Chem. 47 (2012) 97.

JOURNAL PRE-PROOF

[5] A. Sharma, B. Chakravarti, M. P. Gupt, J. A. Siddiqui, R. Konwar, R. P. Tripathi, Bioorg. Med. Chem. 18 (2010) 4711.

[6] M. Valko, C.J. Rhodes, J. Moncol, M. Izakovic, M. Mazur, Chem. Biol. Interact. 160 (2006) 1.

[7] J. Springer, A. Tschirner, K. Hartman, S. Palus, E. K. Wirth, S. B. Ruis, N. Möller, S. von Haehling, J. M. Argiles, J. Köhrle, V. Adams, S. D. Anker, W. Doehner, Int. J. Cancer, 131 (2012) 2187.

[8] I. E. Kibriz, M. Sacmaci, I. Yildirim, S. A. A. Noma, T. Taskin Tok, B. Ates, Arch. Pharm. Chem. Life Sci. 351 (2018) e1800165.

[9] T. Zhang, S. Li, Z. Yi, Q. Wu, F. Meng, Chem. Biol. Drug. Des. 91 (2017) 526.

[10] H. S. Nile, S. Y. Keum, S. A. Nile, J. Biochem. Mol. Toxicol. 32 (2017) e22002.

[11] R. Wang, Y. Lu, S. Wang, J. Med. Chem. 46 (2003) 2287.

[12] K. Okamoto, Y. Kawaguchi, B. T. Eger, E. F. Pai, T. Nishino, J. Am. Chem. Soc. 132 (2010) 17080.

[13] W. Humphrey, A. Dalke, K. Schulten, J. Mol. Graph. 14 (1996) 33.

[14] Schrödinger Release 2018-4: Maestro, Schrödinger, LLC, New York, NY, 2018.

[15] L. Hu, Z. Li, Z. Wang, G. Liu, X. He, X. Wang, C. Zeng, Med. Chem. 11 (2015) 180.

[16] G. Onar, M. O. Karatas, S. Balcıoglu, T. Taskın Tok, C. Gurses, I. Kılıç-Cıkla, N. Özdemir, B. Ates, B. Alıcı, Polyhedron, 153 (2018) 31.

[17] A. P. Sweeney, S. G. Wyllie, R. A. Shalliker, J. L. Markham, J. Ethnopharmacol. 75 (2001) 273.

[18] H. S. Nile, B. Kumar, W. S. Park, Chem. Biol. Drug Des. 82 (2013) 290.

[19] M. D. Hanwell, D. E. Curtis, D. C. Lonie, T. Vandermeersch, E. Zurek, G. R. Hutchison, J. Cheminform. 4 (2012) 1.

[20] T. A. Halgren, J. Comput. Chem. 17 (1996) 490.

JOURNAL PRE-PROOF

JOURNAL PRE-PROOF

[21] G. M. Morris, R. Huey, W. Lindstrom, M. F. Sanner, R. K. Belew, D. S. Goodsell, A. J. Olson, J. Comput. Chem. 30 (2009) 2785.

[22] H. Cao, J. M. Pauff, R. Hille, J. Nat. Prod. 77 (2014) 1693.

[23] G. M. Morris, D. S. Goodsell, S. R. Halliday, R. Huey, W. E. Hart, R. K. Belew, A. J. Olson, J. Comput. Chem. 19 (1998) 1639.

[24] J. A. Erickson, M. Jalaie, D. H. Robertson, R. A. Lewis, M. Vieth, J. Med. Chem. 47 (2004) 45.

JOURNAL PRE-PROOF